

LA-UR-01- 5318

Approved for public release;
distribution is unlimited.

c.1

Title: **ANISOTROPIC DAMAGE ANALYSIS OF HY100 STEEL
UNDER QUASISTATIC LOADING CONDITIONS**

Author(s): Paul J. Maudlin, T-3
Bradford E. Clements, T-1
John B. McKirgan, T-3

Submitted to: *Plasticity 2002 Conference
Aruba ANT
January 3-9, 2002*

LOS ALAMOS NATIONAL LABORATORY



3 9338 00791 1752

Los Alamos

NATIONAL LABORATORY

Los Alamos National Laboratory, an affirmative action/equal opportunity employer, is operated by the University of California for the U.S. Department of Energy under contract W-7405-ENG-36. By acceptance of this article, the publisher recognizes that the U.S. Government retains a nonexclusive, royalty-free license to publish or reproduce the published form of this article, or to allow others to do so, for U.S. Government purposes. Los Alamos National Laboratory requests that the publisher identify this article as work performed under the auspices of the U.S. Department of Energy. Los Alamos National Laboratory strongly supports academic freedom and a researcher's right to publish; as an institution, however, the Laboratory does not endorse the viewpoint of a publication or guarantee its technical correctness.

ANISOTROPIC DAMAGE ANALYSIS OF HY100 STEEL UNDER QUASISTATIC LOADING CONDITIONS

P. J. Maudlin, E. M. Mas, B. E. Clements and J. B. McKirgan

Theoretical Division, Los Alamos National Laboratory, Los Alamos, NM 87545, USA, pjm@lanl.gov, mas@lanl.gov, bclements@lanl.gov, mckirgan@lanl.gov

ABSTRACT- The effect of MnS inclusion orientation on damage evolution and fracture toughness in HY100 steel is investigated in the context of anisotropic damage modeling at the continuum level. Experimental notched-bar data sets are analyzed and modeled using finite element calculations with constitutive behavior that assumes isotropic elastoplastic behavior in conjunction with anisotropic damage.

INTRODUCTION: The presence of a significant volume fraction (0.01% to 1.0%) of MnS ellipsoidal shaped stringers in HY100 and other steels raises the question as to how these defects might affect the mechanical behavior of the bulk material. Presented in Fig. 1a is HY100 unidirectional rolled plate stock that exhibits damage/fracture behavior clearly affected by stringer orientation when quasi-statically loaded in uniaxial tension as notched-bar specimens. The elastoplastic response for this material has been experimentally demonstrated to be isotropic. The loading direction Cauchy stress versus von Mises equivalent strain curves in Fig. 1a show a 30% difference in strain-to-failure when comparing specimens cut and loaded first in the direction of rolling (Case 1) and then cut and loaded in the in-plane transverse direction (Case 2). Figure 1a suggests that the fracture toughness of this steel plate is strongly affected by the initial orientation and shape of the inclusions (30:1 aspect ratio, 30 to 100 μm in length), and possibly by subsequent evolution of shape. In this effort the shape and evolution of these MnS stringers are investigated in the context of a simple continuum treatment based on an underlying isotropic damage model overlaid with a deviatoric formulation for the anisotropic shape effects associated with the inclusions (damage).

APPROACH: A Gurson damage model appropriate for isotropic elastic-plastic ductile materials was developed by Johnson and Addessio [1988] for high-rate deformations. This effort assumed associated flow and used the flow surface:

$$G = \frac{3}{2} \underline{\underline{\sigma}} : \underline{\underline{P}}^d : \underline{\underline{\sigma}} - \sigma^2 \left[1 + q_3 \phi^2 - 2q_1 \phi \cosh \left(\frac{q_2}{2\sigma_s} \underline{\underline{P}}^s : \underline{\underline{\sigma}} : \underline{\underline{I}} \right) \right] = 0 \quad (1)$$

where $\underline{\underline{P}}^s$ and $\underline{\underline{P}}^d$ are spherical and deviatoric projectors, $\underline{\underline{\sigma}}$ is the Cauchy stress for the damaged material, σ is a rate-dependent flow stress, σ_s is a rate-dependent saturation flow stress, ϕ is a scalar damage variable (porosity) and the remaining quantities are material parameters. This formulation also assumed a partition of the rate-of-deformation tensor $\underline{\underline{D}}$ into elastic, plastic and damage parts: $\underline{\underline{D}} = \underline{\underline{D}}^e + \underline{\underline{D}}^p + \underline{\underline{D}}^d$ where $\underline{\underline{D}}^d$ is

spherical in isotropic damage theories. Given that we have this isotropic damage theory based on Eqn. (1) which has been previously cast into a robust algorithm and produces reliable results, we follow the suggestion of Lemaitre and Chaboche [1990] and introduce a second-order diagonal damage tensor $\underline{\underline{\phi}}$ (projected area ratios) which modifies the virgin material stress response $\underline{\underline{\tilde{\sigma}}}$ by a damage effect tensor $\underline{\underline{M}}$ to compute the Cauchy stress for the damaged material: $\underline{\underline{\sigma}} = \underline{\underline{M}}(\underline{\underline{\phi}}) : \underline{\underline{\tilde{\sigma}}}$. We next postulated an evolution law for $\underline{\underline{\phi}}$ whose anisotropic growth is specified via the fourth-order shape tensor $\underline{\underline{J}}$:

$$\dot{\underline{\underline{\phi}}} = \left(\dot{\phi}/\phi\right)_{Gur} \underline{\underline{\phi}} : \underline{\underline{J}} \quad \text{where} \quad \underline{\underline{J}} = \underline{\underline{J}}^{(i)} + \underline{\underline{J}}^{(a)} \quad (2)$$

where for convenience $\underline{\underline{J}}$ can be further partitioned into isotropic and anisotropic parts as indicated in Eqn. (2). Note if $\underline{\underline{J}}^{(i)} = \underline{\underline{P}}^s$ and $\underline{\underline{J}}^{(a)} = \underline{\underline{0}}$ (i.e., take a trace) then Eqn. (2) recovers the Gurson isotropic result. Recalling the physical interpretation of $\underline{\underline{\phi}}$ in terms of damaged and virgin area ratios (Lemaitre and Chaboche [1990]), a kinematical relationship between $\underline{\underline{\phi}}$ and the right-hand damage stretch $\underline{\underline{U}}^d$, and its time derivative, can be derived:

$$\left(\underline{\underline{I}} - \underline{\underline{\phi}}\right) = \underline{\underline{U}}^d \text{Det}\left(\underline{\underline{U}}^d\right)^{-1} \Rightarrow \dot{\underline{\underline{\phi}}} = \left(\underline{\underline{I}} - \underline{\underline{\phi}}\right) \cdot \left[\text{Trace}\left(\underline{\underline{D}}^d\right)\underline{\underline{I}} - \underline{\underline{D}}^d\right] \quad (3a,b)$$

where these tensors are diagonal cast in the basis of the principal axes of the inclusion. The more useful rate-equation for dynamic problems, i.e., Eqn. (3b), follows from multiplicative partition of the deformation gradient into elastic, damage and plastic parts with subsequent application of polar decomposition and time differentiation of the result to derive $\dot{\underline{\underline{U}}^d} = \underline{\underline{U}}^d \cdot \underline{\underline{D}}^d$ under the assumption of negligible plastic and damage spins.

RESULTS AND DISCUSSION: Cauchy stress components in the direction of loading are plotted in Fig. 1b as a function of von Mises equivalent inelastic strain (plastic plus damage strains) for the two Cases defined above where loading is aligned with the 3-axis and 1-axis, respectively; an isotropic Gurson case is also shown for comparison. Stringer growth is constrained in directions of matrix contraction for the two anisotropic cases reflecting the presence of MnS, and is accomplished in the modeling by proper selections of the shape tensor $\underline{\underline{J}}$ that constrains ϕ_{load} to a constant value as shown in Fig. 1b. Figures 2 present shape evolution of the inclusion ellipsoid in terms of the components of $\underline{\underline{U}}^d$ shown in Fig. 2a and components of $\underline{\underline{\phi}}$ shown in Fig. 2b; these results were obtained via integration of the above equations. The Fig. 1b results show only minor differences between the two anisotropic damage cases, albeit both are harder relative to the isotropic Gurson case, and note that larger inelastic strains are evolved for Cases 1 and 2 as more deformation occurs associated with the high aspect ratio ellipsoids. Case 1 shows a ratio evolution of 30:1 (initial condition) increasing to 33:1, whereas for Case 2 the ratio remains constant in the 1-3 and increasing in the 2-3 planes. Given the minor evolution of stringer shape in Figs. 2 in conjunction with the small differences in Cauchy stress in Fig.

1b, the authors conclude that the initial stringer orientation and shape is the key element with respect to the fracture toughness of Fig. 1a, independent of any damage evolution.

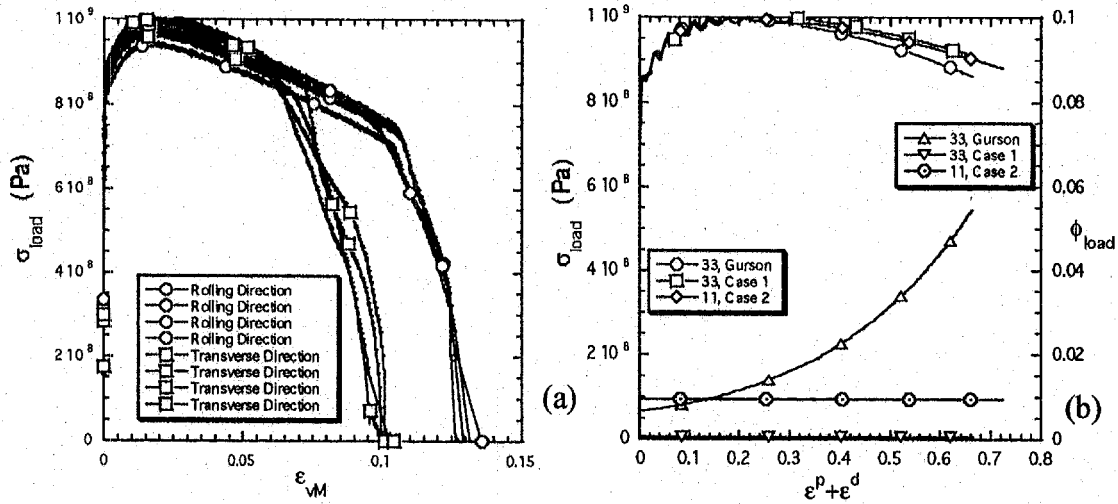


Fig. 1 Uniaxial notch-bar data (a) comparing mechanical response for specimens loaded in the rolling versus the transverse directions. Calculated stress versus inelastic strain response (b) comparing isotropic versus anisotropic inclusion growth for material loaded in the rolling and transverse directions in a state of uniaxial stress.

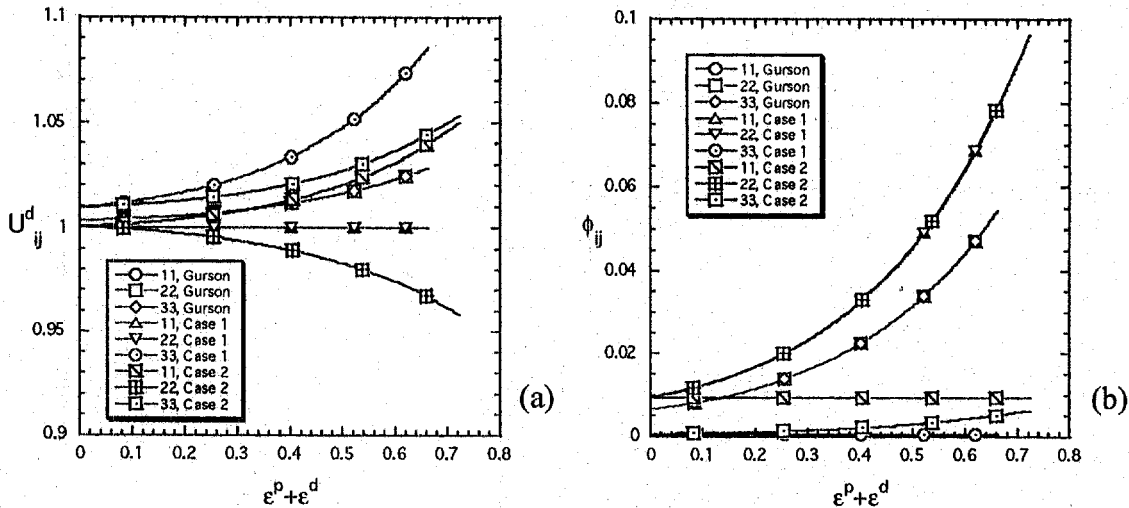


Fig. 2 Evolution of the right-hand damage stretch (a) and damage tensor (b) for uniaxial stress, comparing isotropic damage, anisotropic inclusion growth for material loaded in the rolling and transverse directions in a state of uniaxial stress.

REFERENCES:

- Johnson, J. N. and Addessio, F. L., 1988, "Tensile Plasticity and Ductile Fracture," *J. Appl. Phys.*, **64**, 6699–6712.
 Lemaitre J. and Chaboche J.-L., 1990, *Mechanics of Solid Materials*, Cambridge University Press, Cambridge, UK.